

A continuous-wave $\text{Fe}^{2+} : \text{ZnSe}$ laser

A.A. Voronov, V.I. Kozlovsky, Yu.V. Korostelin, A.I. Landman,
Yu.P. Podmar'kov, Ya.K. Skasyrsky, M.P. Frolov

Abstract. A continuous-wave oscillation is obtained for the first time in a $\text{Fe}^{2+} : \text{ZnSe}$ laser. The laser wavelength was in the range from 4.04 to 4.08 μm . A liquid-nitrogen-cooled active element was pumped by a $\text{Cr}^{2+} : \text{CdSe}$ laser at 2.97 μm . The maximum output power of the laser was 160 mW with the 56% slope efficiency. The minimum absorbed pump power threshold was 18 mW. The intrinsic losses in the $\text{Fe}^{2+} : \text{ZnSe}$ crystal did not exceed 0.024 cm^{-1} during lasing.

Keywords: $\text{Fe}^{2+} : \text{ZnSe}$ laser, cw lasers, IR lasers, solid-state lasers.

1. Introduction

The necessity to develop compact efficient mid-IR lasers arises from a wide range of practical problems that can be solved with the help of such lasers. These problems involve, in particular, the development of various highly sensitive methods for spectral analysis, remote sensing of the atmosphere, monitoring of environment, medicine, etc.

A $\text{Fe}^{2+} : \text{ZnSe}$ crystal belongs to II–VI crystals doped with divalent transition metal ions. These crystals have drawn interest lately as promising active media for tunable mid-IR lasers. Each of these crystals provides continuous tuning over a broad spectral range ($\sim 1000 \text{ cm}^{-1}$), thus ensuring together efficient lasing in the wavelength range from 2 to 5 μm .

The first research in this field of laser physics was initiated by the authors of papers [1, 2], where zinc chalcogenides doped with transition metals were proposed as new active media and lasing in $\text{Cr}^{2+} : \text{ZnSe}$ and $\text{Cr}^{2+} : \text{ZnS}$ crystals was obtained for the first time. Later, cadmium and manganese chalcogenide crystals were investigated. By now, lasing has been obtained in such crystals as $\text{Cr}^{2+} : \text{ZnSe}$ (the obtained tuning range is from 1.88 to 3.1 μm) [3, 4],

$\text{Cr}^{2+} : \text{ZnS}$ (2.17–2.86 μm) [5], $\text{Cr}^{2+} : \text{Cd}_{0.85}\text{Mn}_{0.15}\text{Te}$ (2.30–2.66 μm) [6], $\text{Cr}^{2+} : \text{Cd}_{0.55}\text{Mn}_{0.45}\text{Te}$ (2.17–3.01 μm) [7], $\text{Cr}^{2+} : \text{CdTe}$ (2.54 μm) [8], $\text{Cr}^{2+} : \text{CdSe}$ (2.26–3.61 μm) [9–11] and $\text{Fe}^{2+} : \text{ZnSe}$ (3.77–5.05 μm) [12–15]. However, cw lasing have been obtained so far only in $\text{Cr}^{2+} : \text{ZnSe}$, $\text{Cr}^{2+} : \text{ZnS}$ and $\text{Cr}^{2+} : \text{CdSe}$ crystals with the output powers of 6 W [16], 0.7 W [5] and 1.07 W [17], respectively.

At present, the $\text{Fe}^{2+} : \text{ZnSe}$ laser emits at the longest wavelengths among transition metal ion II–VI crystal lasers. Realisation of continuous-wave generation in the $\text{Fe}^{2+} : \text{ZnSe}$ laser will considerably broaden the scope of its applications. In this paper, we study laser parameters of the Fe^{2+} crystal upon continuous-wave pumping.

2. Preparation of the active element

The active element of the $\text{Fe}^{2+} : \text{ZnSe}$ laser was cut from a $\text{Fe}^{2+} : \text{ZnSe}$ single crystal grown from the vapour phase on a single-crystal seed at 1100–1150 °C by using the concurrent-doping technology which was earlier developed for growing homogeneous single crystals of solid solutions [18, 19]. Advantages of this technology over other methods such as growth from a doped melt or vapor-phase growth of a pure ZnSe crystal followed by the diffusion of Fe through the surface into the crystal are the high structural quality and the high optical homogeneity of grown crystals. As a result, these crystals have low intrinsic losses. The vapour-phase mass transfer was performed by physical transport in helium. The technology is based on the use of separate sources containing ZnSe and FeSe sublimates. By choosing the source geometry, we could control the doping of the vapor phase in a broad concentration range to obtain crystals with the Fe^{2+} concentration from 10^{17} to 10^{19} cm^{-3} . Earlier, we used $\text{Fe}^{2+} : \text{ZnSe}$ crystals grown by this method to obtain efficient pulsed lasing [13–15].

The concentration of Fe^{2+} ions in the active element of the $\text{Fe}^{2+} : \text{ZnSe}$ laser, which was determined from the absorption spectrum by using the absorption cross section of the crystal taken from [12], was $\sim 2.5 \times 10^{18} \text{ cm}^{-3}$. The active element was 7.7 mm in length and had the 4×2.5 -mm cross section. The crystal faces of the active element were not AR coated and the angle between them did not exceed 1° .

3. Experimental setup

The optical arrangement of the experimental setup is shown in Fig. 1. The $\text{Fe}^{2+} : \text{ZnSe}$ crystal was pumped by a cw

A.A. Voronov Moscow Institute of Physics and Technology (State University), Institutskiy per. 9, 141700 Dolgoprudny, Moscow region, Russia;

V.I. Kozlovsky, Yu.V. Korostelin, A.I. Landman, Yu.P. Podmar'kov, Ya.K. Skasyrsky, M.P. Frolov P.N. Lebedev Physics Institute, Russian Academy of Sciences, Leninsky prosp. 53, 119991 Moscow, Russia; e-mail: frolovmp@x4u.lebedev.ru

Received 21 February 2008

Kvantovaya Elektronika 38 (12) 1113–1116 (2008)

Translated by M.V. Politov

$\text{Cr}^{2+}:\text{CdSe}$ laser described in detail in [17]. The $\text{Cr}^{2+}:\text{CdSe}$ laser was pumped by a diode-pumped cw TLM-05LP thulium fibre laser (IRE-Polyus Research and Technology Association) emitting 5 W at 1.908 μm . Because the absorption band of the $\text{Fe}^{2+}:\text{ZnSe}$ crystal had the maximum at $\sim 3 \mu\text{m}$ [12], the $\text{Cr}^{2+}:\text{CdSe}$ laser was tuned, unlike [17], to a wavelength of $\sim 2.97 \mu\text{m}$, by using the output mirror with a specially selected transmission spectrum. The output power of the $\text{Cr}^{2+}:\text{CdSe}$ laser was 0.6 W. The laser operated in the fundamental transverse mode and had the nearly diffraction-limited beam.

The laser action in the $\text{Fe}^{2+}:\text{ZnSe}$ crystal takes place between the ${}^5\text{T}_2$ and ${}^5\text{E}$ states of the Fe^{2+} ions. The lifetime of the upper laser level ${}^5\text{T}_2$ of the Fe^{2+} ion in a ZnSe matrix falls with temperature from $\sim 100 \mu\text{s}$ at 77 K to 5 μs at 220 K [12] and to 370 ns at room temperature [15] due to the increase in the rate of nonradiative relaxation. This results in a rapid increase in the lasing threshold with temperature. For this reason, the active element was mounted on a liquid-nitrogen-cooled copper heatsink inside a cryostat. One of the crystal faces of size $7.7 \times 4 \text{ mm}$ was pressed against the heatsink through an indium layer. One of the cryostat windows was a plane-parallel CaF_2 plate and the other was the output mirror of the $\text{Fe}^{2+}:\text{ZnSe}$ laser.

The resonator of the $\text{Fe}^{2+}:\text{ZnSe}$ laser was formed by a flat highly reflecting mirror M1 and an output spherical ($R = 50 \text{ mm}$) mirror M2. The transmittances of the output mirrors were 2.9%, 10.2%, 17%, and 34.5% at the laser wavelength. The resonator was nearly semiconcentric. The output mirror M2 was fixed in a flange fastened tightly to the cryostat housing with a sylphon, which allowed us to change the length of the laser resonator during its adjustment. The $\text{Fe}^{2+}:\text{ZnSe}$ crystal was mounted 1 mm away from mirror M1 so that its polished faces were perpendicular to the optical axis of the cavity.

The $\text{Fe}^{2+}:\text{ZnSe}$ crystal was pumped along the optical axis of the resonator through the CaF_2 cryostat window and

the mirror M1 with the 97% transmittance at the pump wavelength. The pump beam was focused into a $\sim 150\text{-}\mu\text{m}$ spot to the centre of the $\text{Fe}^{2+}:\text{ZnSe}$ crystal by a CaF_2 lens with a focal distance of 110 mm. The pump power was controlled with the help of calibrated optical filters placed before the lens.

The pump power and the output power of the $\text{Fe}^{2+}:\text{ZnSe}$ laser were measured with Gentec-EO UP19K-15S-W5-D0 (PM1) and IMO-2N (PM2) power meters, respectively. The parameters of the $\text{Fe}^{2+}:\text{ZnSe}$ laser were studied by using two optical filters placed alternately at the laser output. The first filter rejected pump radiation not absorbed in the crystal and was used to measure the output power of the laser. The second filter rejected output radiation of the $\text{Fe}^{2+}:\text{ZnSe}$ laser and was used to measure the fraction of the pump power absorbed in the crystal. The measurements showed that 90% of the pump power were absorbed in the active element during lasing.

A diffraction monochromator with a 1-nm resolution was used to measure the emission wavelength of the $\text{Fe}^{2+}:\text{ZnSe}$ laser.

4. Results

We have obtained continuous-wave lasing in a $\text{Fe}^{2+}:\text{ZnSe}$ crystal for the first time. Figure 2 shows the output power of the laser versus the pump power absorbed in the $\text{Fe}^{2+}:\text{ZnSe}$ crystal for different transmittances of the output mirror $T = 2.9\%$, 10.2%, 17%, 34.5%. The slope efficiencies η of the laser with respect to the absorbed pump power determined from the slopes of straight lines drawn through the experimental points are also presented in Fig. 2.

The maximum efficiency $\eta = 56\%$ was achieved when the transmission of the output mirror was 34.5%. In this case, the maximum output power was 160 mW for the absorbed pump power of 340 mW, and the absorbed threshold pump power of 56 mW. The minimum absorbed

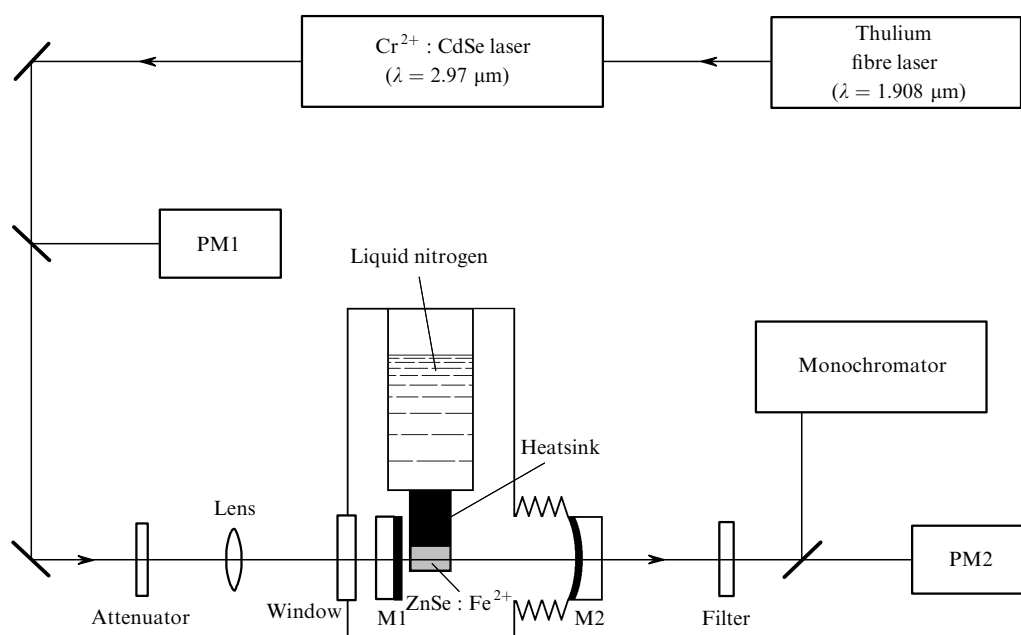


Figure 1. Optical arrangement of the experimental setup: M1, M2 are the resonator mirrors, PM1, PM2 are the power meters.

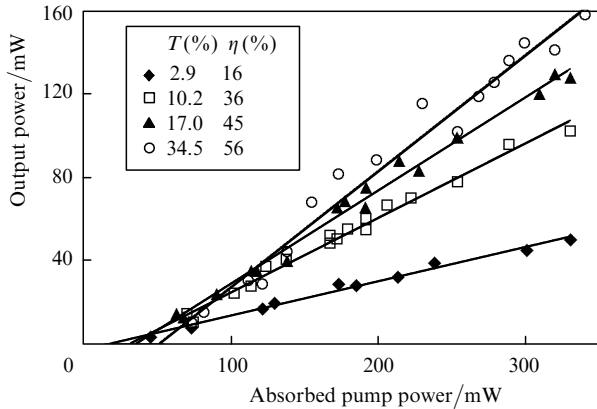


Figure 2. Dependences of the output power of the Fe²⁺:ZnSe laser on the absorbed pump power obtained for different output mirrors with various transmittances T . The slope efficiencies η of the laser with respect to the absorbed pump power are presented for each of the mirrors.

threshold pump power of 18 mW was achieved when the transmission of the output mirror was 2.9%.

The emission spectrum of the Fe²⁺:ZnSe laser depended on the output mirror and lied in the wavelength range from 4.04 to 4.08 μm . The width of this spectrum was ~ 10 nm.

We used the experimental slope efficiencies obtained for four output mirrors to estimate passive intracavity losses with the help of a simple model [20] relating the laser efficiency to the transmission of the output mirror. We took into account that when the crystal working surface faces the output mirror perpendicular to the resonator optical axis, a Fabry–Perot interferometer formed by mirror M2 with the reflectance $1 - T$ and by the face of the Fe²⁺:ZnSe crystal with the Fresnel reflectance $R_F = 17\%$ serves, in fact, as the output mirror of the Fe²⁺:ZnSe laser. The minimum transmittance T_{FP} of this interferometer is described by the expression [21]

$$T_{FP} = \frac{T(1 - R_F)}{\{1 + [(1 - T)R_F]^{1/2}\}^2}, \quad (1)$$

It follows from (1) that T_{FP} is 1.2%, 4.3%, 7.3%, and 15.9% for the output mirror described above.

According to [20], we can write

$$\frac{1}{\eta} = \frac{1}{\eta_0} + \frac{L}{\eta_0} \frac{1}{T_{FP}} \quad (2)$$

Relation (2) is used to determine the total passive losses L per round trip in the cavity and the limiting laser efficiency η_0 :

$$\eta_0 = \frac{\lambda_p}{\lambda_g} \eta_p \left(1 - \frac{\sigma_{ESA}}{\sigma}\right), \quad (3)$$

where λ_p is the pump wavelength; λ_g is the laser wavelength; η_p is the pump efficiency; σ_{ESA} is the cross section of the excited-state absorption; σ is the laser transition cross section.

Figure 3 shows the dependence of $1/\eta$ on $1/T_{FP}$, from which we found $\eta_0 = 67\%$ and $L = 3.7\%$. The found value of η_0 is close to the maximum laser efficiency 73%, which is determined by the ratio of the energies of laser and pump

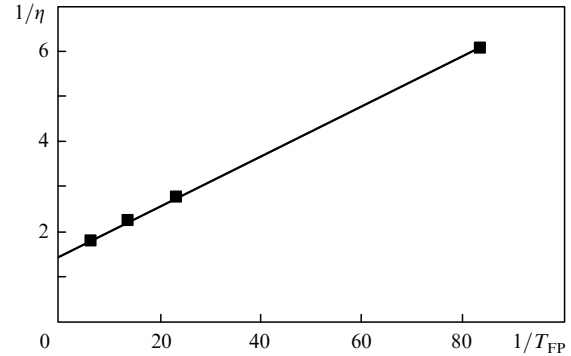


Figure 3. Dependence of the inverse efficiency on the inverse transmission $1/T_{FP}$ of the Fabry–Perot interferometer formed by the output resonator mirror and the ZnSe:Fe²⁺ crystal surface facing it.

photons. This demonstrates a weak excited-state absorption and good matching between the pump region and the mode volume of the laser cavity.

The quantity L includes total losses of laser radiation per round trip in the cavity, namely, diffraction losses, light scattering on resonator mirrors and crystal faces, and, also, absorption in the crystal itself. Taking into account that the experimental value of L is 3.7% and assuming that the total losses are determined only by intrinsic losses in the crystal, we determined that the absorption coefficient at the laser wavelength is 0.024 cm^{-1} , which proves a high quality of the optical element.

5. Conclusions

We have obtained for the first time continuous-wave lasing in the Fe²⁺:ZnSe laser, which has the longest emission wavelength among lasers based on II–VI crystals doped with divalent transition metal ions. The output power of the laser has reached 160 mW for the 56% slope efficiency of the absorbed pump power. Taking into account the ratio of the energies of the laser and pump photons, this corresponds to the quantum slope efficiency of 76%.

An important feature of this paper is the fact that the Fe²⁺:ZnSe crystal was pumped by a Cr²⁺:CdSe laser based on a II–VI crystal doped with divalent transition metal ions.

The maximum output power of the Fe²⁺:ZnSe laser was limited in our experiments by the power of the Cr²⁺:CdSe laser and pump radiation losses in the feed optics. Apparently, the output power can be significantly increased with increasing the pump power of the source and using AR-coated optical elements for transporting and focusing pump radiation.

Acknowledgements. This work was supported by the grant of the RF President for the State Support of Leading Scientific Schools (Grant No. NSh-6055.2006.02), by the Fundamental Research Program of Physical Sciences Department of RAS ‘Coherent Optical Radiation of Semiconductor Compounds and Structures’, by the Program of the RF Ministry of Education and Science ‘Development of Scientific Potential of Higher School’, the Program of the RAS Presidium ‘Procurement of Scientific Devices and Equipment’, and ‘Reagent’ Science and Technology Center.

References

1. DeLoach L.D., Page R.H., Wilke G.D., Payne S.A., Krupke W.F. *IEEE J. Quantum Electron.*, **32**, 885 (1996).
2. Page R.H., Schaffers K.I., DeLoach L.D., Wilke G.D., Patel F.D., Tassano J.B., Payne S.A., Krupke W.F., Chen K.-T., Burger A. *IEEE J. Quantum Electron.*, **33**, 609 (1997).
3. Sorokina I.T. *Opt. Mater.*, **26**, 395 (2004).
4. Demirbas U., Sennaroglu A. *Opt. Lett.*, **31**, 2293 (2006).
5. Sorokina I.T., Sorokin E., Mirov S., Fedorov V., Badikov V.V., Panyutin V., Schaffers K.I. *Opt. Lett.*, **27**, 1040 (2002).
6. Seo J.T., Hömmerich U., Trivedi S.B., Chen R.J., Kutcher S. *Opt. Commun.*, **153**, 267 (1998).
7. Trivedi S.B., Kutcher S.W., Wang C.C., Jagannathan G.V., Hömmerich U., Bluiett A., Turner M., Seo J.T., Schepler K.L., Schumm B., Boyd P.R., Green G. *J. Electron. Mater.*, **30**, 728 (2001).
8. Bluiett A., Hömmerich U., Shah R.T., Trivedi S.B., Kutcher S.W., Wang C.C. *J. Electron. Mater.*, **31**, 806 (2002).
9. McKay J., Schepler K.L., Catella G.C. *Opt. Lett.*, **24**, 1575 (1999).
10. McKay J., Roh W.B., Schepler K.L. *Techn. Dig. Conf. on Advanced Solid-State Lasers* (Quebec, OSA, 2002) Paper WA7.
11. Akimov V.A., Kozlovsky V.I., Korostelin Yu.V., Landman A.I., Podmar'kov Yu.P., Skasyrsky Ya.K., Frolov M.P. *Kvantovaya Elektron.*, **38**, 205 (2008) [*Quantum Electron.*, **38**, 205 (2008)].
12. Adams J.J., Bibeau C., Page R.H., Krol D.M., Furu L.H., Payne S.A. *Opt. Lett.*, **24**, 1720 (1999).
13. Voronov A.A., Kozlovsky V.I., Korostelin Yu.V., Landman A.I., Podmar'kov Yu.P., Frolov M.P. *Kvantovaya Elektron.*, **35**, 809 (2005) [*Quantum Electron.*, **35**, 809 (2005)].
14. Akimov V.A., Voronov A.A., Kozlovsky V.I., Korostelin Yu.V., Landman A.I., Podmar'kov Yu.P., Frolov M.P. *Kvantovaya Elektron.*, **36**, 299 (2006) [*Quantum Electron.*, **36**, 299 (2006)].
15. Fedorov V.V., Mirov S.B., Gallian A., Badikov V.V., Frolov M.P., Korostelin Yu.V., Kozlovsky V.I., Landman A.I., Podmar'kov Yu.P., Akimov V.A., Voronov A.A. *IEEE J. Quantum Electron.*, **42**, 907 (2006).
16. Mirov S., Fedorov V., Moskalev I., Martyshkin D. *IEEE J. Sel. Top. Quantum Electron.*, **13**, 810 (2007).
17. Akimov V.A., Kozlovsky V.I., Korostelin Yu.V., Landman A.I., Podmar'kov Yu.P., Skasyrsky Ya.K., Frolov M.P. *Kvantovaya Elektron.*, **37**, 991 (2007) [*Quantum Electron.*, **37**, 991 (2007)].
18. Korostelin Yu.V., Kozlovsky V.I., Nasibov A.S., Shapkin P.V. *J. Cryst. Growth*, **159**, 181 (1996).
19. Korostelin Yu.V., Kozlovsky V.I. *J. Alloys Compounds*, **371**, 25 (2004).
20. Caird J.A., Payne S.A., Staver P.R., Ramponi A.J., Chase L.L., Krupke W.F. *IEEE J. Quantum Electron.*, **24**, 1077 (1988).
21. Gagarinsky S.V., Galagan B.A., Denker B.A., Korchagin A.A., Osiko V.V., Prikhodko K.V., Sverchkov S.E. *Kvantovaya Elektron.*, **30**, 10 (2000) [*Quantum Electron.*, **30**, 10 (2000)].